Lyapunov vectors and assimilation in the unstable subspace: Theory and applications

Article *in* Journal of Physics A Mathematical and Theoretical · June 2013

DOI: 10.1088/1751-8113/46/25/254020

CITATIONS
48

READS
279

3 authors:

Luigi Palatella
Liceo Scientifico Statale "C. De Giorgi" Lecce (ITALY)
97 PUBLICATIONS **1,602** CITATIONS
SEE PROFILE

A. Carrassi
University of Reading
78 PUBLICATIONS **1,852** CITATIONS
SEE PROFILE

Anna Trevisan
Italian National Research Council
56 PUBLICATIONS **1,135** CITATIONS
SEE PROFILE

Lyapunov vectors and assimilation in the unstable subspace: theory and applications

2013 J. Phys. A: Math. Theor. 46 254020

(http://iopscience.iop.org/1751-8121/46/25/254020)

J. Phys. A: Math. Theor. **46** (2013) 254020 (19pp) doi:10.1088/1751-8113/46/25/254020

Lyapunov vectors and assimilation in the unstable subspace: theory and applications

Luigi Palatella[1], **Alberto Carrassi**[2] **and Anna Trevisan**[3]

[1] Istituto di Scienze dell'Atmosfera e del Clima del CNR ISAC-CNR, UOS di Lecce, Str. Prov. Lecce-Monteroni km 1200, I-73100 Lecce, Italy
[2] Institut Catalá de Ciéncies del Clima—IC3, Carrer del Doctor Trueta, 203, E-08005 Barcelona, Spain
[3] Istituto di Scienze dell'Atmosfera e del Clima del CNR ISAC-CNR, via P Gobetti 101, I-40129 Bologna, Italy

E-mail: luigi.palatella@yahoo.it, alberto.carrassi@ic3.cat and a.trevisan@isac.cnr.it

Received 1 July 2012, in final form 3 October 2012
Published 4 June 2013
Online at stacks.iop.org/JPhysA/46/254020

Abstract
Based on a limited number of noisy observations, estimation algorithms provide a complete description of the state of a system at current time. Estimation algorithms that go under the name of assimilation in the unstable subspace (AUS) exploit the nonlinear stability properties of the forecasting model in their formulation. Errors that grow due to sensitivity to initial conditions are efficiently removed by confining the analysis solution in the unstable and neutral subspace of the system, the subspace spanned by Lyapunov vectors with positive and zero exponents, while the observational noise does not disturb the system along the stable directions. The formulation of the AUS approach in the context of four-dimensional variational assimilation (4DVar-AUS) and the extended Kalman filter (EKF-AUS) and its application to chaotic models is reviewed. In both instances, the AUS algorithms are at least as efficient but simpler to implement and computationally less demanding than their original counterparts. As predicted by the theory when error dynamics is linear, the optimal subspace dimension for 4DVar-AUS is given by the number of positive and null Lyapunov exponents, while the EKF-AUS algorithm, using the same unstable and neutral subspace, recovers the solution of the full EKF algorithm, but dealing with error covariance matrices of a much smaller dimension and significantly reducing the computational burden. Examples of the application to a simplified model of the atmospheric circulation and to the optimal velocity model for traffic dynamics are given.

This article is part of a special issue of *Journal of Physics A: Mathematical and Theoretical* devoted to 'Lyapunov analysis: from dynamical systems theory to applications'.

PACS numbers: 05.45.−a, 05.45.Gg, 05.45.Pq

(Some figures may appear in colour only in the online journal)

1. Introduction

The problem of estimating the state of an evolving system from an incomplete set of noisy observations is the central theme of the classical estimation and optimal control theory [1, 2]. A natural field of applications has been in experimental and applied physics in general as well as in engineering, where the aim is to extract as much information as possible about a natural or laboratory-scale phenomenon on the basis of a limited amount of noisy observations.

A relevant domain of application has been in the context of numerical weather and oceanic prediction, where it is usually referred to as *data assimilation* [2, 3]. The ultimate goal there is to provide the best possible estimate of an unknown system's state by using all the information available [4]. Data assimilation algorithms have experienced a flourishing stream of development in geoscience, where they are used for diagnostic purposes and to provide the initial condition, *the analysis*, for weather and climate prediction. The analysis is obtained by merging, under some optimal criteria, the information coming from the model and observations.

In sequential assimilation the system's state estimate, given by a solution of the model equations, is updated at each time when observations are available. It is well known that in the case of a linear dynamics, and a linear relation between observations and the system's state variables, the filtering problem can be expressed via the Kalman filter (KF) equations [5, 1]. For nonlinear dynamics, an extension of the KF formulation has been proposed, the extended Kalman filter (EKF) [1], which has been largely studied in geophysical contexts [6, 7]. In the EKF the system state evolves according to the full nonlinear dynamics, while the associated error covariance is propagated in time through the linearized dynamics. As long as the dynamics of the error is well approximated by the tangent linear equations, the EKF has proved to be quite efficient [7] while preserving one of the most attractive features of the KF equations, namely the time propagation of the error covariance, which is desirable especially in the case of chaotic dynamics where the error evolution is conditioned by the local instabilities of the flow.

An alternative approach is referred to as variational. The state estimation in the variational assimilation is formulated as an optimal control problem, and aims at determining the trajectory which best fits the observations and accounts for the dynamical constraints given by the equations governing the flow. The accuracy of the variational solution is naturally connected to our knowledge of the error associated with the information sources.

The dynamics of most natural systems of interest is chaotic and characterized by a huge number of degrees of freedom. For instance, atmospheric and oceanic observations are noisy and much scattered in space and time; the dynamical models used to simulate their evolution are chaotic and their number of degrees of freedom is huge ($>10^9$). The chaotic character of the real systems and forecast models has two important implications. One is the need to provide an accurate estimate of the initial state to stretch the range of valuable forecasts towards the systems' predictability limits. The other, more subtle consequence of the growth of the initial uncertainty is that the state estimation error itself strongly projects on the unstable manifold of the forecast model [8].

Many authors have stressed the importance of the unstable manifold in chaotic dynamics, but only recently has this concept been investigated in the context of the state estimation problem for chaotic systems: while all assimilation methods, more or less implicitly, exert some control on the flow-dependent instabilities, algorithms referred to as assimilation in the unstable subspace (AUS) exploit the unstable subspace, the span of the leading Lyapunov vectors, as key dynamical information in the assimilation process. The AUS approach, originally introduced in [9] and developed by Trevisan and co-workers, consists in confining the analysis update

in the subspace spanned by the leading unstable directions. Applications to atmospheric and oceanic models [10, 11] showed that even dealing with high-dimensional systems, an efficient error control can be obtained by monitoring only a limited number of unstable directions.

AUS has been recently incorporated and formalized in the framework of the variational and EKF approaches [12, 13]: the information on the unstable and neutral manifolds is explicitly used in the algorithm setup. By confining the state estimate correction to the unstable and neutral manifolds, the AUS formulations turn out to be as efficient as but much less computationally demanding than their standard counterparts, a very attractive feature in geoscience data assimilation. Most importantly, the series of successful applications of AUS demonstrate the robustness of its fundamental paradigm: an efficient error control can be achieved by monitoring only a limited number of well-chosen dynamically relevant phase-space directions. This number is approximately equal to the dimension of the unstable and neutral subspace.

This paper is structured as follows. First an overview of the data assimilation formalism and notation is provided in section 2, with a focus on the specific procedure suitable for applications in nonlinear dynamics. The AUS algorithm is outlined in section 3, while its variational and EKF formulations, along with the corresponding numerical results, are presented in sections 4 and 5, respectively. Concluding remarks and a discussion on ongoing research directions are given in section 6.

2. Data assimilation: basic concepts and definitions

Let us consider the problem of estimating the state of a discrete dynamical system given by

$$\mathbf{x}_{k+1} = \mathcal{M}_{k\to k+1}(\mathbf{x}_k), \quad k = 0, 1, 2, \ldots, \tag{1}$$

where the state at t_k is an n-vector. The distribution $\mathcal{P}(\mathbf{x}_0)$ of the initial conditions is assumed given. Let discrete noisy observations $\mathbf{y}_k^o$ be given by

$$\mathbf{y}_k^o = \mathcal{H}(\mathbf{x}_k) + \varepsilon_k^o, \quad k = 1, 2, \ldots, \tag{2}$$

where $\mathbf{y}_k^o$ is a p-vector ($p \ll n$ in many applications), ε_k^o is a white Gaussian error sequence, $\mathcal{N}(0, \mathbf{R}_k)$, independent of $\mathbf{x}_0$ and $\mathcal{H}$ is the observation operator mapping from model to observed variables. Now let $\mathbf{Y}_l^o$ be the sequence of observations:

$$\mathbf{Y}_l^o = \mathbf{y}_1^o, \mathbf{y}_2^o, \ldots \mathbf{y}_l^o. \tag{3}$$

Given a realization of the sequence of observations $\mathbf{Y}_l^o$, the problem consists in computing an estimate of $\mathbf{x}_k$. For $k < l$, $k = l$, $k > l$ the problem is referred to as smoothing, filtering and prediction, respectively.

In the probabilistic approach, the conditional probability density function (PDF) of $\mathbf{x}_k$:

$$\mathcal{P}\big(\mathbf{x}_k|\mathbf{Y}_l^o\big), \quad l = 1, 2, \ldots k \tag{4}$$

given $\mathbf{Y}_l^o$ and $\mathcal{P}(\mathbf{x}_0)$ are the complete solution to the filtering problem. Given the correct initial PDF and assuming that the properties of the observational noise are known, the PDF's time evolution could in principle be predicted using the Fokker–Planck equation. In practice, in the nonlinear high-dimensional case it is impossible to determine the complete PDF, let alone compute its time evolution.

The problem simplifies enormously in the presence of linear dynamics and Gaussian errors. The PDFs are fully characterized by the first two moments, the mean and the covariance, and by maximizing the conditional PDF, one obtains the solution that minimizes the posterior error variance:

$$\mathcal{E}\big\{\big(\mathbf{x}_k - \mathbf{x}_k^t\big)^T \mathbf{S}\big(\mathbf{x}_k - \mathbf{x}_k^t\big)\big\}, \tag{5}$$

where $\mathbf{x}^t$ is the *true* state, $\mathcal{E}\{\}$ is the expectation operator and $\mathbf{S}$ is a positive definite matrix. Under these conditions, the minimum error variance estimate coincides with the conditional mean $\mathcal{E}\{\mathbf{x}_k^t|\mathbf{Y}_k^o\}$.

The KF provides a self-consistent framework for the state estimation in linear systems affected by Gaussian errors. The KF belongs to the family of the sequential schemes (see [6, 3] and references therein): the state estimate is propagated between observation times along with the associated error covariance according to

$$\mathbf{x}^a = \mathbf{M}\mathbf{x}^f \tag{6}$$

and

$$\mathbf{P}^f = \mathbf{M}\mathbf{P}^a\mathbf{M}^T, \tag{7}$$

with $\mathbf{x}^f$ ($\mathbf{P}^f$) and $\mathbf{x}^a$ ($\mathbf{P}^a$) being the forecast and the analysis state (error covariance), respectively, while $\mathbf{M}$ is the linear dynamical model.

When observations become available, the state and error covariance estimates are updated through

$$\mathbf{x}^a = \mathbf{x}^f - \mathbf{K}\mathbf{H}\mathbf{x}^f + \mathbf{K}\mathbf{y}^o, \tag{8}$$

and

$$\mathbf{P}^a = (\mathbf{I} - \mathbf{K}\mathbf{H})\mathbf{P}^f, \tag{9}$$

respectively, where $\mathbf{H}$ is the linear observation operator and $\mathbf{K}$ is the Kalman gain matrix given by [1]:

$$\mathbf{K} = \mathbf{P}^f\mathbf{H}^T(\mathbf{H}\mathbf{P}^f\mathbf{H}^T + \mathbf{R})^{-1}. \tag{10}$$

In all the above equations the time index has been dropped to simplify the notation.

In contrast with the sequential procedures, the variational approach aims at the statistical estimate of the model solution over a specified assimilation interval. The statistical approach gives the same solution, the best linear unbiased estimate, as the probabilistic approach, provided the weighting matrices reflect the correct properties of the error statistics [1]. The solution of the variational problem is obtained by minimizing, with respect to $\mathbf{x}_0, \ldots, \mathbf{x}_K$, a cost function measuring the misfit with observations and some *a priori* estimate $\mathbf{x}_0^b$ at the beginning of the assimilation interval:

$$J = \left(\mathbf{x}_0 - \mathbf{x}_0^b\right)^T\mathbf{B}^{-1}\left(\mathbf{x}_0 - \mathbf{x}_0^b\right) + \sum_{k=0}^{K}\left(\mathcal{H}(\mathbf{x}_k) - \mathbf{y}_k^o\right)^T\mathbf{R}_k^{-1}\left(\mathcal{H}(\mathbf{x}_k) - \mathbf{y}_k^o\right) \tag{11}$$

subject to the constraint given by the model equation (1); $\mathbf{y}_k^o$ are the observations available at discrete times $t_k = k\Delta t$, $k = 0, \ldots, K$, within the assimilation window of length $\tau = t_K - t_0$ and $\mathcal{H}$ is the (possibly) nonlinear observation operator. Note that in the cost function (11), the model is assumed to be perfect and is appended as a strong constraint when solving for the extremes of (11); when this hypothesis is relaxed, a term accounting for the model error appears and it gives rise to the so-called weak-constraint four-dimensional variational (4DVar) formulation [14, 15].

The positive definite matrices $\mathbf{B}^{-1}$ and $\mathbf{R}^{-1}$ are to be regarded as *weighting* matrices, quantitative measures of our belief in the prior estimate, $\mathbf{x}_0^b$ and the observations. In 4DVar, $\mathbf{x}_0^b$ can be a model forecast from a previous analysis as in the KF, the important difference being that in the KF its associated error covariance estimate $\mathbf{P}^f$, that plays the role of $\mathbf{B}$, is sequentially obtained from previous analysis steps (equations (7) and (9)).

In practical applications of 4DVar, observations are collected in *batches* or *observation windows* to solve the problem separately for each *batch* of observations. Information from one batch is carried over to the next batch via the first term in the cost function which must be prescribed at $t = t_0$.

2.1. Data assimilation algorithms for nonlinear dynamics

In most realistic applications, particularly in environmental science, the model equations are nonlinear. Nonlinear estimation can be simplified by assuming that the error dynamics is linear: the EKF and 4DVar described below are the most notable examples of sequential and variational algorithms of this sort.

The EKF is a straightforward way of extending the KF equations to the nonlinear case [1, 7]: the state estimate is evolved using the nonlinear model, equation (1), but the linearized model is used to propagate the error covariance between two successive analysis times according to equation (7). When observations become available they are assimilated through the KF analysis update, equations (8) and (9), and provide the new analysis state and error covariance.

4DVar is an advanced technique that seeks the model trajectory that best fits the observations distributed within a given time interval with the dynamical constraint of the model equations [16]. By assuming that the model is perfect and deterministic, the adjoint technique [17] allows the minimization of the 4DVar cost function to be made with respect to the state at the beginning of the interval. The solution of the minimization problem is obtained by forward integration of the model and backward integration of the adjoint of the tangent linear propagator that enters the expression of the cost function gradient. Given the same initial estimates of the background state and of the background error covariance, if errors are Gaussian and small enough to be described by the tangent linear equations, 4DVar and EKF give the same solution.

Some general comments are in place at this point. First of all it needs to be stressed that, in real-world applications, the validity of the linear hypothesis depends on different factors: the characteristics of the observation network, the frequency and accuracy of observations, the error growth rate and the properties of the assimilation scheme. In 4DVar, the length of the time window is another parameter that must be controlled. Second, what really matters is the asymptotic performance of the assimilation scheme. In KF-like filters, the error covariance matrix is updated at each step along the assimilation-forecast cycle and the asymptotic performance of the filter is independent of the guess of the error covariance at time $t = t_0$. In addition, the evolved error covariance matrix in the KF provides a measure of the goodness of the estimate. However, the computational cost of the error covariance propagation in the full EKF is prohibitively expensive in most relevant applications let alone for NWP models. In 4DVar, the error covariance $\mathbf{B}$ associated with the background state at the beginning of each assimilation window must be prescribed and the asymptotic performance depends, among other factors, on the accuracy of this estimate. However it is often computed statistically and then kept fixed and it does not reflect the time-dependent behaviour of the actual error. Provided the errors are small, 4DVar and EKF would give the same results if either $\mathbf{B} = \mathbf{P}^f$ or the assimilation window is long enough so that 4DVar loses memory about the initial $\mathbf{B}$. However the difficulty is to fulfil these conditions in practice.

The reader is referred to [3, 18] for a review on the state of the art of data assimilation in geoscience; see also [19–21] for a discussion on the relative merits of 4DVar and KFs.

3. Data assimilation for unstable dynamics

The nonlinear stability properties of the system do not only determine the predictability horizon of the initial value problem but also profoundly influence the assimilation process, affecting directly its quality and that of the subsequent forecast. If a system is chaotic, only by means of observations is it possible to keep the estimate from diverging from the true trajectory. In

this section we first provide the basic definitions of Lyapunov vectors, along with some details on the techniques suitable for their numerical estimation, and introduce then the AUS which makes an explicit use of these unstable directions.

3.1. Basic definitions of Lyapunov vectors

The stability of an aperiodic orbit is studied by considering the evolution along the flow of infinitesimal perturbations. The dynamics is described by the tangent linear equations and defines the tangent space of the nonlinear trajectory. Lyapunov vectors can be considered as the generalization of the eigenmodes of a fixed point and Floquet vectors of a periodic orbit. Lyapunov vectors are norm independent and covariant with the dynamics, i.e. a vector associated with a given exponent at a given point is mapped by the tangent linear equations into its image at any subsequent point along the nonlinear trajectory. The span of Lyapunov vectors with positive, null and negative exponents defines the unstable, neutral and stable manifolds of the system. Because in general Lyapunov vectors are not orthogonal to one another, their numerical computation is not straightforward. Computing the subspaces spanned by a given number of Lyapunov vectors is obtained efficiently by performing recurrent orthonormalization [22], but computing the individual vectors themselves requires the use of complex numerical algorithms that involve the intersections of subspaces obtained by forward and backward orthonormalization, i.e. proceeding in a direct or reverse order with respect to the order of the exponents (see e.g. [23]). This procedure is not computationally affordable for high-dimensional systems and several authors have suggested ways to overcome this difficulty [24, 25]; for a review of recently developed algorithms for the computation of Lyapunov vectors of high-dimensional systems, see [26].

3.2. The assimilation in the unstable subspace

The basic idea of confining the AUS can be easily understood when errors behave linearly, that is when there are enough and sufficiently accurate observations, the estimate remains at all times close to the true state. Then its evolution can be described in terms of the evolution of the Lyapunov directions, with suitable projection coefficients. During the forecast, errors in the directions with positive (negative) Lyapunov exponents will amplify (decay). When the forecast is combined with the observations to form the analysis, error components that have amplified will be reduced; only if the observations are perfect, can these components be reduced to zero. Forecast errors in decaying directions naturally tend to zero if not sustained by an observational error. By confining the analysis increment only in the unstable and neutral subspace, with the AUS approach it is thus possible to keep the estimated trajectory close to the true trajectory, at least in a perfect model setting.

The first applications of the AUS assimilation dealt with the problem of selecting the locations, which depend on the particular state of the system, of supplementary observations meant to achieve the greatest improvement in analysis and forecasts. This problem was one of the research challenges undertaken by the international program of THORPEX (the observing system research and predictability experiment) to accelerate the improvement in high impact weather forecasting: additional observations could be *adaptively* located in geographical regions where the fixed observations were not sufficient to control the growth of errors due to flow-dependent instabilities.

The error in an assimilation-forecast cycle is expected to depend on the structure, growth and propagation properties of flow instabilities, as well as on the temporal and geographical distribution of observations. These errors can be most efficiently reduced by tracking the

structure of the errors in the most unstable directions that develop along the trajectory and by placing observations in the locations where the maximum amplitude of the structure is attained. By confining the analysis increment in the subspace $\mathbf{E}$ spanned by the most unstable vectors, the analysis solution reads

$$\mathbf{x^a} = \mathbf{x^b} + \mathbf{E\Gamma E}^T\mathbf{H}^T(\mathbf{R} + \mathbf{HE\Gamma E}^T\mathbf{H}^T)^{-1}(\mathbf{y}^o - \mathbf{Hx^b}) \tag{12}$$

with the background covariance matrix $\mathbf{B} = \mathbf{E\Gamma E}^T$ [9]. The most efficient and *safe* (for reasons related to the stability of the solution) way of exploiting just a few unstable directions is to use AUS in combination with observations located where each column of $\mathbf{E}$ attains its maximum value.

In the application to a quasi-geostrophic model with 14 784 degrees of freedom, only a single unstable mode was used to identify optimal locations for adaptive observations: this mode was estimated using breeding on the data assimilation system [27], an approach based on the original breeding technique introduced by Toth and Kalnay [28, 29].

More recently, Trevisan *et al* [12] formulated a reduced subspace four-dimensional assimilation algorithm, four-dimensional variational assimilation in the unstable subspace (4DVar-AUS). The key result of this study is the existence of an optimal subspace dimension for the assimilation that is approximately equal to the unstable and neutral subspace dimension. This subspace, the span of the Lyapunov vectors with positive and null exponents, is the subspace where instabilities develop along the system's trajectory and usually has a dimension much smaller than the total number of degrees of freedom. For instance, Carrassi *et al* [11] find that in a quasi-geostrophic model with 14 784 degrees of freedom, the number of positive exponents is equal to 24.

In recent works, Trevisan and Palatella [13, 30] investigated the consequences of the existence of an unstable manifold for the EKF solution. They presented a mathematically rigorous algorithm that solves the KF equations when all degrees of freedom are considered. They showed that the asymptotic rank of the EKF error covariance matrices is equal to the dimension of the unstable and neutral subspace. As a consequence, the full EKF and a reduced-order algorithm extended Kalman filter assimilation in the unstable subspace (EKF-AUS) with assimilation increments limited to the unstable and neutral subspace were shown to produce the same results. Theoretical and numerical results from these two studies are reviewed in sections 4 and 5.

4. Four-dimensional variational assimilation and its reduction to the unstable subspace

4DVar seeks the model trajectory that best fits the observations available within a given assimilation window. Within the assimilation window, the flow-dependent instabilities are implicitly tracked by the tangent linear propagator, but at the start of each assimilation window, an *a priori* estimate of the background error covariance is required [31].

For long assimilation windows, 4DVar analysis errors are known to project on the unstable subspace of the system [8]. Errors in the stable directions that would be damped in the long range for short assimilation windows are non-negligible in the analysis and affect the next assimilation cycle, causing short-term enhanced error growth as noted in [32] and discussed in [12]. It is possible to avoid introducing errors in the stable directions if we confine the analysis increment in the unstable and neutral subspace of the system; this is obtained by applying to 4DVar the AUS assimilation constraint. As explained below, the dynamical information on the growth of errors in the unstable and neutral directions, the Lyapunov vectors with positive and null exponents, is explicitly estimated in the 4DVar-AUS algorithm [12] and the adjoint

integration is not needed. In the presence of observational noise, the 4DVar-AUS solution is more accurate than the standard 4DVar solution.

The strong constraint 4DVar seeks the (nonlinear) best estimate of the initial state $\mathbf{x}_0$ which minimizes the misfit with observations available in a given time interval (assimilation window) and with a background state $\mathbf{x}_0^b$. The standard cost function for the strong constraint 4DVar, in a discrete form, can be written as in equation (11) with $\mathbf{B}$ and $\mathbf{R}$ representing the background and observation error covariance matrices, $\mathcal{H}$ the nonlinear observation operator and the sequence of model states $\mathbf{x}_k$ is a solution of the nonlinear model equations (1). The adjoint technique allows for the minimization to be done with respect to the model state $\mathbf{x}_0$ at the beginning of the assimilation window. The gradient of J with respect to $\mathbf{x}_0$ can be written as

$$\frac{1}{2}\nabla_{\mathbf{x}_0} J = \mathbf{B}^{-1}\big(\mathbf{x}_0 - \mathbf{x}_0^b\big) + \sum_{k=0}^{K} \mathbf{M}_{0\to k}^T \mathbf{H}_k^T \mathbf{R}^{-1}(\mathcal{H}_k \mathbf{x}_k - \mathbf{y}_k), \tag{13}$$

where $\mathbf{H}_k$ represents the linearized observation operator, and the superscript T stands for transpose.

For a given nonlinear trajectory, the gradient can be estimated by the use of the adjoint method. The solution of the minimization problem is obtained by forward integration of the model and backward integration of the adjoint, with an iterative descent algorithm.

4.1. The 4DVar-AUS algorithm

The 4DVar-AUS algorithm consists in confining the increment $\delta\mathbf{x}_0$ which minimizes the cost function in the reduced dimension subspace spanned by the N most unstable directions of the system corresponding to the leading N Lyapunov exponents. When $N = n$ the full space standard 4DVar solution is recovered.

Let $\mathbf{E}_0$ be the matrix whose columns are the orthonormal tangent vectors spanning the N-dimensional most unstable subspace of the system at t_0, i.e. the orthonormal set of the leading Lyapunov vectors. The linear evolution within the assimilation window $[t_0, t_0 + \tau]$ is given by

$$\mathbf{M}_{0\to k}\mathbf{E}_0 = \mathbf{E}_k \mathbf{\Lambda}_k, \quad k = 0, \ldots, K, \tag{14}$$

where

$$\mathbf{\Lambda}_k = \operatorname{diag}\big[\Lambda_k^{(1)}, \Lambda_k^{(2)}, \ldots, \Lambda_k^{(N)}\big]. \tag{15}$$

$\mathbf{E}_k^j$ are normalized evolved vectors in the time interval j and $\Lambda_k^{(j)}$ is the corresponding jth local amplification factor. The Gram–Schmidt orthonormalization is applied only at $t = t_0$. Let the increment $\delta\mathbf{x}_0$ be confined in the subspace $\mathbf{E}_0$ and its projection $\widetilde{\delta\mathbf{x}_0}$ be given by

$$\widetilde{\delta\mathbf{x}_0} = \mathbf{E}_0\mathbf{E}_0^T\delta\mathbf{x}_0, \tag{16}$$

where for simplicity, the Euclidean norm is adopted. The evolution of the projected increment is governed by

$$\widetilde{\delta\mathbf{x}_k} = \mathbf{M}_{0\to k}\mathbf{E}_0\mathbf{E}_0^T\delta\mathbf{x}_0 = \mathbf{E}_k\mathbf{\Lambda}_k\mathbf{E}_0^T\delta\mathbf{x}_0, \quad k = 0, \ldots, K. \tag{17}$$

The cost function gradient in the reduced subspace can be written as

$$\frac{1}{2}\widetilde{\nabla_{\mathbf{x}_0} J} = \mathbf{E}_0\left[\mathbf{E}_0^T\mathbf{B}^{-1}\big(\mathbf{x}_0 - \mathbf{x}_0^b\big) + \sum_{k=0}^{K}\mathbf{\Lambda}_k\mathbf{E}_k^T\mathbf{H}_k^T\mathbf{R}^{-1}(\mathcal{H}_k\mathbf{x}_k - \mathbf{y}_k)\right]. \tag{18}$$

The minimization proceeds as in the 4DVar algorithm (for details, see [12]) and in the assimilation cycle the estimated state and its associated unstable subspace are used to initialize the next assimilation window. Note that no use of the adjoint integration is made. In the 4DVar-AUS assimilation, N is approximately equal to the number of positive and null Lyapunov exponents, N^+ and N^0, respectively.

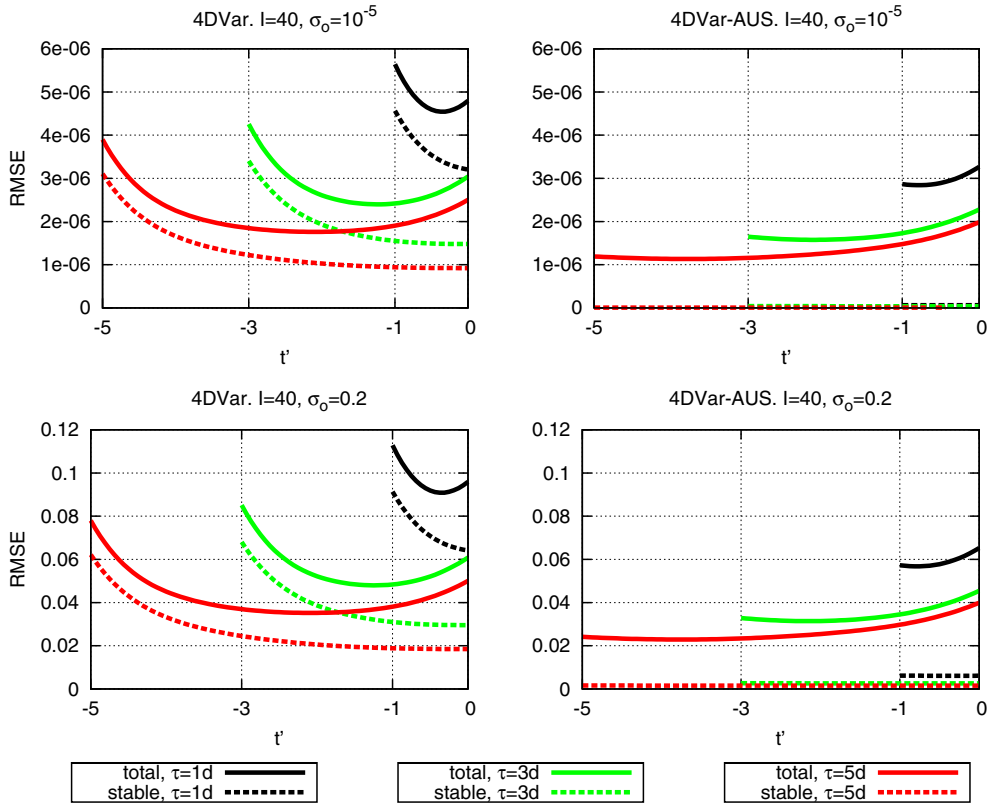

Figure 1. After [12]. Time-averaged RMS error within one-, three- and five-day assimilation windows as a function of $t' = t - \tau$, with $\sigma_o = 0.2, 10^{-5}$ for the model configuration $n = 40$. *Left panel*: 4DVar. *Right panel*: 4DVar-AUS with $N = 15$. Solid lines refer to total assimilation error; dashed lines refer to the error component in the stable subspace.

4.2. 4DVar-AUS results

To illustrate the behaviour of the algorithm, model [33] is used. The model describes the evolution of a meteorological variable around a circle at equal latitude. We refer to [12] for the specific model setup adopted here. Numerical experiments were performed with three different configurations (40, 60 and 80 longitudinal grid points). The number of positive exponents $N^+ = 13, 19, 26$ in the three configurations is proportional to the spatial extension of the domain. The unstable and neutral subspace, the span of Lyapunov vectors with positive or null exponents, contains the most rapidly growing perturbations: 4DVar-AUS confines the assimilation of observations in this subspace. In standard 4DVar, errors at the beginning (end) of the assimilation window tend to be confined in the stable (unstable) subspace for long assimilation windows [8]. In 4DVar-AUS, after a certain number of iterations of the assimilation cycle, errors are confined in the unstable subspace both at the beginning and at the end of the assimilation window (see figure 1).

Furthermore, the error of 4DVar-AUS is smaller than the error of 4DVar, particularly for short assimilation windows, when the errors in the stable directions do not have enough time to be damped and affect the 4DVar solution also at the end of the window. One of the main

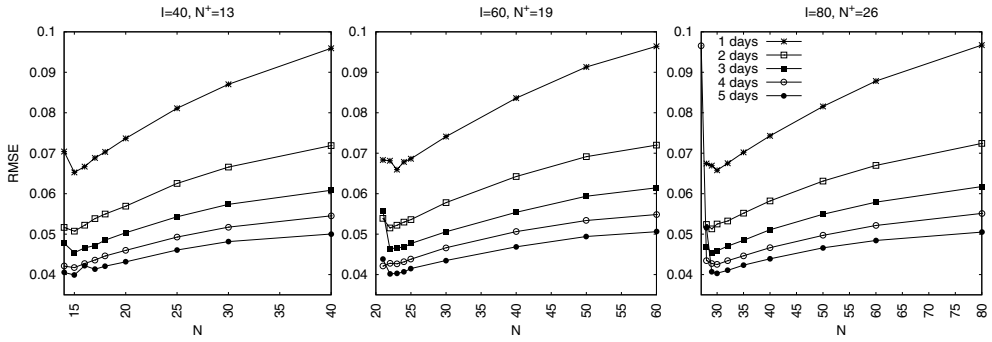

Figure 2. After [12]. Time-averaged RMS analysis error at $t = \tau$ as a function of the subspace dimension N for three model configurations: $n = 40, 60, 80$. Different curves in the same panel refer to different assimilation windows from one to five days. The observation error standard deviation is $\sigma_o = 0.2$.

results of the study was to find that, in the presence of observational error, there is an optimal subspace dimension for the assimilation that is approximately equal to $N^+ + N^0$ (see figure 2).

The 4DVar solution that minimizes the cost function in the whole space ($N = n$), while closer to the observations, is farther away from the truth. This result has been explained showing that, when assimilating in the unstable and neutral subspace, errors in the stable directions are naturally damped. Because of the observational error, assimilating in the whole space otherwise keeps the stable components of the error alive, deteriorating the overall assimilation performance.

5. The EKF and its reduction to the unstable subspace

In the EKF, the propagation of the flow-dependent instabilities is obtained by explicitly evolving the analysis error covariance estimate from the previous analysis step: the dimension of the error covariance matrices is equal to the state dimension, n. In a reduced form, referred to as EKF-AUS, the assimilation is performed in the unstable and neutral subspace of the tangent space of dimension N and the rank of the error covariance matrices is equal to N.

5.1. The EKF-AUS algorithm

The algorithm belongs to the family of square-root implementations of the EKF [34, 35]. The assimilation is performed in a manifold of dimension N. When N is equal to the total number of degrees of freedom of the system, the algorithm solves the standard EKF equations. When $N = N^+ + N^0$, the reduced form with AUS (EKF-AUS) is obtained.

At time $t = t_{k-1}$ (here and in the following we drop the time-step subscript from the equations given that, except for $\mathbf{X}^a$ and equation (19), all terms refer to the same time step k), let the columns of the $n \times N$ matrix $\mathbf{X}^a = [\mathbf{x}_1^a, \mathbf{x}_2^a, \ldots, \mathbf{x}_N^a]$ be orthogonal with $\mathbf{X}^a$ one of the square roots of $\mathbf{P}^a$, namely:

$$\mathbf{P}^a = \mathbf{X}^a \mathbf{X}^{aT}. \tag{19}$$

At time $t = t_0$, the vectors $\mathbf{x}_i^a$, $i = 1, 2, \ldots, N$ are arbitrary independent initial perturbations. In the standard EKF algorithm, the number of perturbations is equal to the total number of degrees of freedom of the system, $N = n$.

The forecast step. In the forecast step, the tangent linear operator $\mathbf{M}$ acts on the perturbations $\mathbf{X}^a$ defined at (analysis) time $t = t_{k-1}$: $\mathbf{X}^f = \mathbf{M}\mathbf{X}^a$, where $\mathbf{X}^f = [\mathbf{x}_1^f, \mathbf{x}_2^f, \ldots, \mathbf{x}_N^f]$. The $n \times n$ forecast error covariance matrix $\mathbf{P}^f$ can be cast in the form

$$\mathbf{P}^f = \mathbf{X}^f \mathbf{X}^{fT} \equiv \mathbf{E}^f \mathbf{\Gamma}^f \mathbf{E}^{fT}, \tag{20}$$

where the N columns of $\mathbf{E}^f$ are obtained by a Gram–Schmidt orthonormalization of the columns of $\mathbf{X}^f$. The $N \times N$ (in general non-diagonal) symmetric matrix $\mathbf{\Gamma}^f$ defined as

$$\mathbf{\Gamma}^f = \mathbf{E}^{fT} \mathbf{X}^f \mathbf{X}^{fT} \mathbf{E}^f \tag{21}$$

represents the forecast error covariance matrix, confined to the subspace $\mathcal{S}^N$ of the evolved perturbations.

The analysis step. Using the definition of $\mathbf{P}^f$ of equation (20), the Kalman gain (10) becomes

$$\mathbf{K} = \mathbf{E}^f \mathbf{\Gamma}^f (\mathbf{H}\mathbf{E}^f)^T [(\mathbf{H}\mathbf{E}^f)\mathbf{\Gamma}^f (\mathbf{H}\mathbf{E}^f)^T + \mathbf{R}]^{-1} \tag{22}$$

and the usual analysis error covariance update equation (9) reads

$$\begin{aligned} \mathbf{P}^a &= (\mathbf{I} - \mathbf{K}\mathbf{H})\mathbf{E}^f \mathbf{\Gamma}^f \mathbf{E}^{fT} \\ &= \mathbf{E}^f \mathbf{\Gamma}^f \mathbf{E}^{fT} - \mathbf{E}^f \mathbf{\Gamma}^f (\mathbf{H}\mathbf{E}^f)^T \left[(\mathbf{H}\mathbf{E}^f)\mathbf{\Gamma}^f (\mathbf{H}\mathbf{E}^f)^T + \mathbf{R}\right]^{-1} \mathbf{H}\mathbf{E}^f \mathbf{\Gamma}^f \mathbf{E}^{fT} \\ &= \mathbf{E}^f \{\mathbf{\Gamma}^f - \mathbf{\Gamma}^f \mathbf{E}^{fT} \mathbf{H}^T [(\mathbf{H}\mathbf{E}^f)\mathbf{\Gamma}^f (\mathbf{H}\mathbf{E}^f)^T + \mathbf{R}]^{-1} \mathbf{H}\mathbf{E}^f \mathbf{\Gamma}^f\} \mathbf{E}^{fT} \\ &\equiv \mathbf{E}^f \mathbf{\Gamma}^{a'} \mathbf{E}^{fT}. \end{aligned} \tag{23}$$

The analysis error covariance matrix $\mathbf{P}^a$ can be written as

$$\mathbf{P}^a = \mathbf{E}^f \mathbf{\Gamma}^{a'} \mathbf{E}^{fT} = \mathbf{E}^f \mathbf{U} \mathbf{\Gamma}^a \mathbf{U}^T \mathbf{E}^{fT} \equiv \mathbf{E}^a \mathbf{\Gamma}^a \mathbf{E}^{aT}, \tag{24}$$

where the columns of the $(N \times N)$ orthogonal invertible matrix $\mathbf{U}$ are the eigenvectors of the symmetric matrix $\mathbf{\Gamma}^{a'} = \mathbf{U}\mathbf{\Gamma}^a\mathbf{U}^T$ and $\mathbf{\Gamma}_a = \mathrm{diag}[\gamma_i^2]$ is diagonal. Therefore, the N columns of $\mathbf{E}^a = [\mathbf{e}_1^a, \mathbf{e}_2^a, \ldots, \mathbf{e}_N^a]$ obtained by

$$\mathbf{E}^a = \mathbf{E}^f \mathbf{U} \tag{25}$$

span the same subspace $\mathcal{S}^N$ as the columns of $\mathbf{E}^f$. Consequently, the analysis step preserves the subspace $\mathcal{S}^N$, an important point for the discussion below on the comparison of our scheme with Benettin *et al*'s algorithm [22]. The square root of $\mathbf{P}^a$, written as $\mathbf{P}^a = \mathbf{E}_a \mathbf{\Gamma}_a \mathbf{E}_a^T = \mathbf{X}_a \mathbf{X}_a^T$, provides a set of orthogonal vectors:

$$\mathbf{X}^a = \mathbf{E}^a (\mathbf{\Gamma}^a)^{1/2}. \tag{26}$$

The columns of

$$\mathbf{X}^a = \left[\gamma_1 \mathbf{e}_1^a, \gamma_2 \mathbf{e}_2^a, \ldots, \gamma_m \mathbf{e}_N^a\right] = \left[\mathbf{x}_1^a, \mathbf{x}_2^a, \ldots., \mathbf{x}_N^a\right] \tag{27}$$

are the new set of perturbation vectors defined after the analysis step at time t_k that enter the forecast step at the next time step t_{k+1}. When $N = n$, $\mathbf{K}$ is the usual Kalman gain (10). In EKF-AUS ($N = N^+ + N^0$), the analysis increment is confined to the subspace $\mathcal{S}^N$ spanned by the N columns of $\mathbf{E}^f$ in view of the form of $\mathbf{K}$.

The authors of [13, 30] compared the steps in the evolution of perturbations in the EKF algorithm with those of the procedure of [22] to compute orthonormalized Lyapunov vectors. As shown above, in the assimilation cycle, the analysis step preserves the subspace and reduces the amplitude of the perturbations, while the forecast perturbations $\mathbf{X}^f$ are repeatedly orthogonalized but not orthonormalized. Thus, in the long run, perturbations in the stable directions will decay and only the unstable and neutral subspace Lyapunov vectors will, in the end, be the same as those computed in Benettin *et al*'s [22] algorithm. Therefore the EKF and EKF-AUS algorithms will asymptotically produce the same estimate of error covariances and the two algorithms will be equivalent as confirmed by numerical experiments described in sections 5.2 and 5.3.

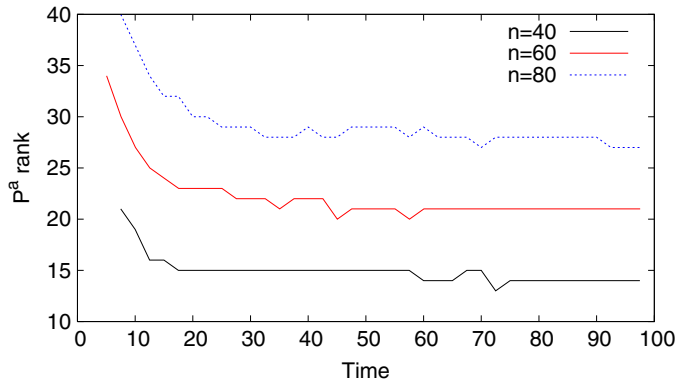

Figure 3. After [13]. Rank of the analysis error covariance matrix $\mathbf{P}^a$ in the EKF algorithm. For $n = 40, 60, 80$, the dimension of the unstable and neutral space is $14, 20, 26$, respectively. $\sigma_0 = 0.01$.

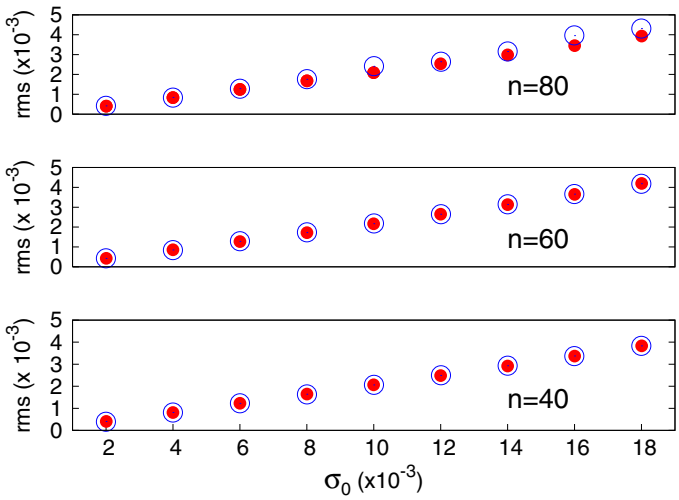

Figure 4. After [13]. Average root mean square error of the algorithms: EKF (full circles), EKF-AUS (empty circles) for systems with $n = 40, 60, 80$ degrees of freedom. The average was performed over 1000 assimilation steps.

5.2. EKF-AUS results: atmospheric dynamics

As in the '4DVar-AUS results' section, to illustrate the behaviour of the algorithm the atmospheric model [33] is used. The same model configuration as in [13] is used here. Numerical experiments were performed with three different configurations (40, 60 and 80 longitudinal grid points). The number of positive exponents is 13, 19 and 26, respectively.

The results confirm the theoretical prediction that the rank of $\mathbf{P}^a$ in the full EKF decays in time and asymptotically becomes as small as the dimension of the number of positive and null Lyapunov exponents of the original system (figure 3). This is because only the estimated errors in the unstable and neutral subspace survive the filtering process.

Another key result confirmed by the numerical experiments is that the full EKF and its reduced form EKF-AUS give the same results: the average rms error (figure 4) and

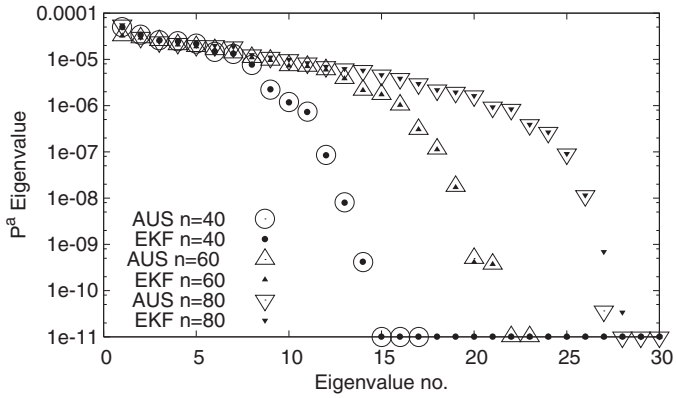

Figure 5. After [13]. Eigenvalues of the analysis error covariance matrix at final time of assimilation with: EKF (full) and EKF-AUS (empty) for systems with $n = 40, 60, 80$. $\sigma_0 = 0.01$.

the eigenvalues of the asymptotic analysis covariance matrix (figure 5) are in fact the same.

It should be stressed that all considerations regarding the behaviour of the error estimate are valid in the framework of EKF theory based on the assumption that errors behave linearly. If errors do not behave linearly, the EKF will still provide the same error estimate, but the true error may not be confined in the unstable and neutral subspace but live in a higher dimensional subspace. In that case, as indicated by numerical results, in order to avoid filter divergence it may be necessary to artificially augment the subspace of the estimated error, in analogy with the findings of 4DVar-AUS study [12]. If observational and estimation errors are not too big, we found that it is sufficient to augment the dimension of the tangent subspace of the EKF-AUS, N, of just a few units [13]. The 4DVar-AUS and EKF-AUS studies indicate that the proper, minimum subspace for the assimilation is the unstable and neutral subspace. The theoretical result that its dimension is a relevant parameter has important implications also for the design of the ensemble-based data assimilation algorithms. This result is confirmed by some recent studies: in the context of deterministic filters, and under the hypothesis of small errors, it was found that the optimal ensemble size (i.e. the minimum size required to efficiently constraint the estimation error below the observational error level) is equal to or slightly larger than the number of unstable modes of the dynamics [36, 37]. Similarly Ng *et al* [38] have shown, in the context of the ensemble KF, that divergence is avoided only if the full linearized long-term unstable subspace is spanned by the ensemble members.

5.3. EKF-AUS results: traffic dynamics

This section describes the results of the application of the EKF-AUS algorithm in the context of a traffic dynamical model. The model, referred to in the literature as the microscopic intelligent driver *optimal velocity* (OV) traffic model, is a deterministic dynamical system, where the motion of individual vehicles is described by second-order ordinary differential equations for the position and the velocity (see [39] and references therein). In its simplest version, the OV model describes the motion of vehicles in a single-lane road stretch or a circular circuit, but it can be used in more complex road networks. We refer to [39] for the specific choices of relevant model parameters such as the 'optimal velocity', i.e. the speed a driver will adopt to maintain a given safety distance.

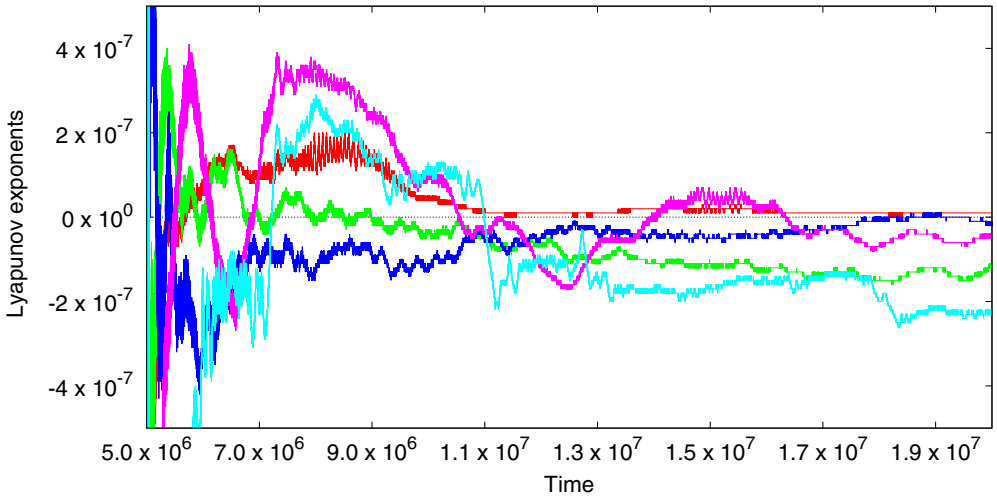

Figure 6. Leading five Lyapunov exponents, for the OV model, as a function of time t. The sixth to eighth computed exponents are in the range -10^{-7} to -10^{-5}.

As explained in [39] the choice of boundary conditions has important consequences on the resulting dynamics and on its stability. Periodic boundary conditions are used to simulate traffic in a circular road with a fixed number of vehicles in the circuit. Empirical boundary conditions are used to prescribe the inflow of vehicles, obtained by adding a new vehicle at the beginning of a highway stretch (as it enters from the left) with free outflow of vehicles at its (right) end. In such a case, the total number of vehicles is variable and is determined by the internal dynamics and by the, possibly stochastic, prescription of their inflow.

In this paper we present results obtained with periodic boundary conditions. The following values for the relevant parameters in the experiments have been selected: length of the domain is 200 corresponding to 1 km in real units; the number of cars is 150. The adimensional units for time, space and velocity correspond to $1/6$ s, 5 m and 30 m s^{-1}, respectively. Computation of the spectrum of Lyapunov exponents revealed that the non-negative exponents have a very slow convergence to their asymptotic value. The exponents decay very slowly and, as shown in figure 6, they are asymptotically zero or negative. In the case considered, with a number of cars $C = 150$ we observe for the largest time of the computation (2×10^7) that only one exponent has a very small positive value, followed by three exponents with very small negative values. Given that the OV equations are autonomous, the system has at least one null Lyapunov exponent. Moreover, since the periodic boundary conditions give an exact translational symmetry, we conclude that the system has two null Lyapunov exponents whose degeneracy prevents a full numerical convergence of Benettin *et al*'s algorithm [22]. This conclusion is strengthened by the results of the assimilation experiments which suggest that the OV model is not chaotic.

The structure of the Lyapunov vectors (shown in figure 7) has a close correspondence with the spatial organization of the flow and lends them a qualitative interpretation. Lyapunov vectors show sharp velocity peaks with a positive (negative) sign at the boundaries between stops and go's in correspondence with high state velocity gradients[4]; the vectors' displacement

[4] Like other microscopic traffic models, the OV model, under suitable choice of parameters, presents an unstable uniform state. Arbitrary small perturbations grow and the uniform state is completely lost. The system then evolves towards a state with portion of the road filled with cars at rest (the stops) separated by zones with cars moving with a similar velocity (the go's). The length of stops and go's is approximately the same.

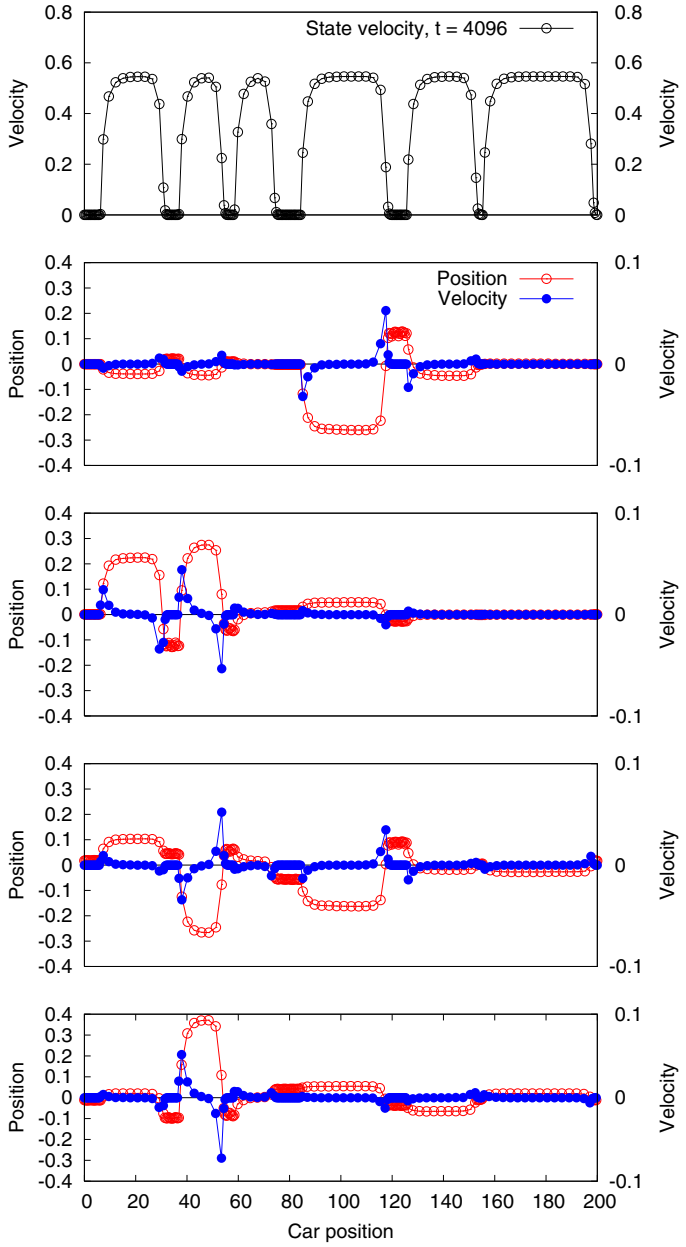

Figure 7. From top to bottom. *Uppermost panel*: state vector velocity field at time $t = 4096$ as a function of the car positions. Leading four non-orthogonal Lyapunov vectors at time $t = 4096$ as a function of the car positions; lines with empty (red) circles and full (blue) circles refer to position and velocity and are reported on the left and right sides of the y-axis, respectively.

in position has the same spatial extension as that of the stop or go ahead and, as a natural consequence, it has the same sign as the vector velocity peak. We note that, as observed by [23] in a different dynamical system, the Lyapunov vectors here are very similar to the Floquet vectors computed in [40].

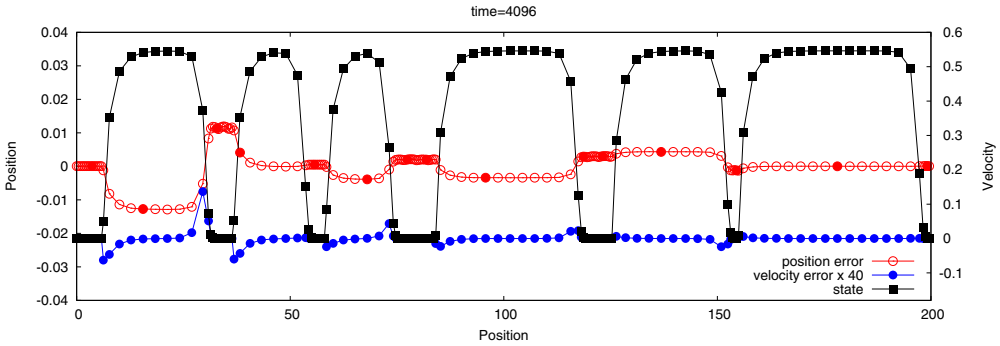

Figure 8. State vector (lines with squares) and actual analysis error (difference between 'analysis' and 'truth' fields) at time $t = 4096$ as function of the cars' position. As in figure 7 lines with empty (red) and full (blue) circles refer to position and velocity and are reported on the left and right sides of the y-axis, respectively. Note that the velocity values have been multiplied by 40 to improve visualization.

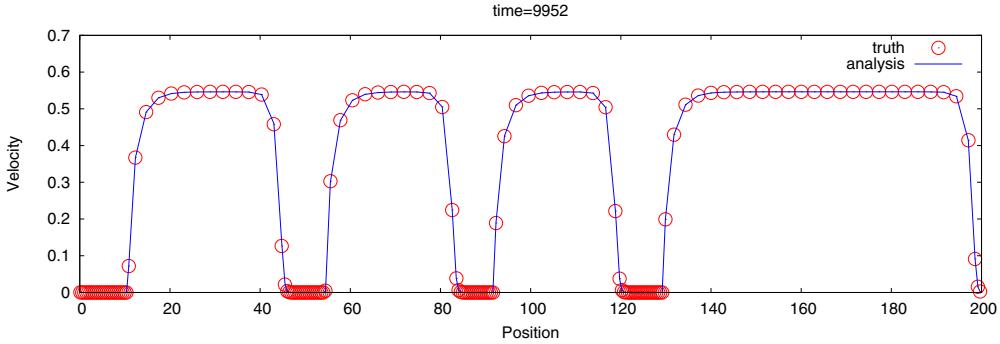

Figure 9. Analysis velocity field (blue line) along with the true field (red empty circles) at time $t = 9952$ as a function of the cars' positions.

Assimilation experiments are performed with the OV model assuming that a small percentage of the cars are monitored: the error standard deviation in position and velocity is $\sigma_o = 0.01$ in adimensional units, corresponding to 5 cm and 0.3 m s^{-1}, respectively, typical values of real GPS measurements. The EKF-AUS algorithm, with a number of perturbations $N = 3$, is applied and results obtained by monitoring one-tenth of the cars are shown in figure 8.

By comparing figures 7 and 8 we see that as expected, the structures of the Lyapunov vectors and of the analysis error have similar features. They are both constant in space inside each stop and go while the velocity error is localized in the transitions between them.

Even if we monitor only one over ten cars, the actual error, the difference between the analysis and the true state, does not show significant difference between the monitored and non-monitored cars. This is due to the fact that the Lyapunov vectors closely reflect the actual error covariance, particularly within each stop and go group of cars.

The assimilation experiments are performed with $N = 3$ perturbations and increasing this value does not significantly improve the results. Figure 9 shows the analysis velocity field along with the true field at time $t = 9952$: the accuracy of the tracking of the truth provided by the EKF-AUS is evident. The average (on all the cars) analysis error (0.0031) is rather smaller than the observation error.

6. Conclusions

Data assimilation constitutes nowadays a central part of operational weather and climate prediction and has attracted attention from a wide range of different research domains such as astrophysics, biology and transport infrastructure management, among others. The reasons for this growth of interest are connected to the development of advanced observing/measurement facilities, the increase in computational power and the refinement of the knowledge of the fundamental processes of given natural or human-driven phenomena of interest. Data assimilation offers the concepts and algorithms to properly take advantage of all these ingredients to provide a more accurate picture of the system under study.

The assimilation in the unstable subspace (AUS) is an advanced data assimilation approach which makes explicit use of the unstable and neutral manifolds of the dynamics in order to efficiently spread the information content of the observations. The basic paradigm relies on the existence of such an unstable/neutral manifold and on its typical reduced dimension with respect to the full phase space where the dynamics takes place. Under these hypotheses, which usually hold for the large class of dissipative chaotic systems present in nature, novel assimilation algorithms have been developed and applied in a set of different model and observational scenarios.

This study reports about two competitive formulations of AUS, which have recently appeared in the literature, in the framework of variational and sequential schemes. Results from applications in the context of simple prototypes of atmospheric and traffic dynamics are presented. Overall the numerical analysis demonstrated the efficiency of AUS in maximizing the information content by monitoring only a limited number of phase-space directions, much less than the full phase-space dimension. The highest accuracy of the AUS formulation is accompanied by a significant reduction of the computational cost compared to the standard procedures and, in the case of variational schemes, there is the further advantage that the adjoint model is no longer required. Another relevant practical feature is that AUS algorithms embed the automatic selection of the time-dependent unstable modes and the only information one has to introduce is an overestimate of their number.

The AUS theory has been derived under the hypothesis of the perfect model so that the origin of the estimation uncertainty is the (growth of the) initial condition error only and the source of noise are the observations alone. It is easy to understand that these conditions do not strictly fit in most realistic applications, where the models at disposal are usually only an approximate representation of the actual dynamics. Data assimilation is nowadays confronted with the problem of accounting for the model error in the assimilation procedures. Studying the extension of the AUS formalisms in the presence of model error and understanding the limits of its applicability depending on the model deficiencies are a relevant line of research in progress (Talagrand, private communication).

Another challenge is data assimilation in the presence of multiple-scale instabilities. The emergence of multiple scales of motions is inherently connected with the refinement of the modelling capabilities, with the increase in computational power (which allows for an increase in the model resolution) with the use of coupled models built on sub-models possessing very different scales of motions. The latter situation is typical in long-term climate predictions where atmospheric general circulation models are coupled to an ocean model (but other components are usually included such as, for instance, a soil and a sea-ice model).

The existing data assimilation algorithms are not adequate to simultaneously control the growth of errors due to small-scale fast growing and large-scale slower unstable modes. Facing this scenario with the AUS approach is also worth being analysed. Based on dynamical arguments we believe that there is room for the AUS scheme to be successful under these

circumstances, as long as an efficient practical way to identify the unstable modes on the selected scales is implemented and observations of the same scales are available.

Acknowledgments

This work was partly financed by the *Centro Interdipartimentale 'L. Galvani' Per Studi Integrati di Bioinformatica, Biofisica e Biocomplessità* through the Project Pegasus Ind.2015. AC was financed through the IEF Marie Curie Project 'INCLIDA' of the FP7.

References

[1] Jazwinski A H 1970 *Stochastic Processes and Filtering Theory* (New York: Academic)
[2] Daley R 1991 *Atmospheric Data Analysis* (Cambridge: Cambridge University Press)
[3] Kalnay E 2003 *Atmospheric Modeling, Data Assimilation and Predictability* (Cambridge: Cambridge University Press)
[4] Talagrand O 1997 Assimilation of observations, an introduction *J. Meteorol. Soc. Japan* **75** 191–209
[5] Kalman R 1960 A new approach to linear filtering and prediction problems *Trans. ASME* D **82** 3545
[6] Ghil M and Malanotte-Rizzoli P 1991 Data assimilation in meteorology and oceanography *Adv. Geophys.* **33** 141–266
[7] Miller R N, Ghil M and Gauthier F 1994 Advanced data assimilation in strongly nonlinear dynamical systems *J. Atmos. Sci.* **51** 1037–56
[8] Pires C, Vautard R and Talagrand O 1996 On extending the limits of variational assimilation in nonlinear chaotic systems *Tellus* A **48** 96–121
[9] Trevisan A and Uboldi F 2004 Assimilation of standard and targeted observations within the unstable subspace of the observation-analysis-forecast cycle system *J. Atmos. Sci.* **61** 103–13
[10] Uboldi F and Trevisan A 2006 Detecting unstable structures and controlling error growth by assimilation of standard and adaptive observations in a primitive equation ocean model *Nonlinear Process. Geophys.* **16** 67–81
[11] Carrassi A, Trevisan A, Descamps L, Talagrand O and Uboldi F 2008 Controlling instabilities along a 3DVar analysis cycle by assimilating in the unstable subspace: a comparison with the EnKF *Nonlinear Process. Geophys.* **15** 503–21
[12] Trevisan A, D'Isidoro M and Talagrand O 2010 Four-dimensional variational assimilation in the unstable subspace and the optimal subspace dimension *Q. J. R. Meteorol. Soc.* **136** 487–96
[13] Trevisan A and Palatella L 2011 On the Kalman filter error covariance collapse into the unstable subspace *Nonlinear Process. Geophys.* **18** 243–50
[14] Tremolet Y 2007 Model-error estimation in 4D-Var *Q. J. R. Meteorol. Soc.* **133** 1267–80
[15] Carrassi A and Vannitsem S 2010 Accounting for model error in variational data assimilation: a deterministic formulation *Mon. Weather Rev.* **138** 3369–86
[16] Talagrand O and Courtier P 1987 Variational assimilation of observations with the adjoint vorticity equations *Q. J. R. Meteorol. Soc.* **113** 1311–28
[17] Le Dimet F X and Talagrand O 1986 Variational algorithms for analysis and assimilation of meteorological observations—theoretical aspects *Tellus* **38** 97–110
[18] Tsuyuki T and Miyoshi T 2007 Recent progress of data assimilation methods in meteorology *J. Meteorol. Soc. Japan* B **85** 331–61
[19] Lorenc A C 2003 The potential of the ensemble Kalman filter for NWP—a comparison with 4DVAR *Q. J. R. Meteorol. Soc.* **129** 3183–293
[20] Kalnay E, Li H, Miyoshi T, Yang S-C and Ballabrera-Poy J 2007 4DVar or ensemble Kalman filter? *Tellus* A **59** 758–73
[21] Gustafsson N 2007 Discussion on '4DVar or EnKF'? *Tellus* A **59** 774–7
[22] Benettin G, Galgani L, Giorgilli A and Strelcyn J M 1980 Lyapunov characteristic exponents for smooth dynamical systems and for Hamiltonian systems, a method for computing them *Meccanica* **15** 9–21
[23] Trevisan A and Pancotti F 1998 Periodic orbits, Lyapunov vectors, and singular vectors in the Lorenz system *J. Atmos. Sci.* **55** 390–8
[24] Ginelli F, Poggi P, Turchi A, Chatè H, Livi R and Politi A 2007 Characterizing dynamics with covariant Lyapunov vectors *Phys. Rev. Lett.* **99** 130601

[25] Wolfe C L and Samelson R M 2007 An efficient method for recovering Lyapunov vectors from singular vectors *Tellus* A **59** 355–66
[26] Kuptsov P V and Parlitz U 2012 Theory and computation of covariant Lyapunov vectors *J. Nonlinear Sci.* **22** 727–62
[27] Carrassi A, Trevisan A and Uboldi F 2007 Adaptive observations and assimilation on the unstable subspace by breeding on the data assimilation system *Tellus* A **59** 101–13
[28] Toth Z and Kalnay E 1993 Ensemble forecasting at NMC: the generation of perturbations *Bull. Am. Meteorol. Soc.* **74** 2317–30
[29] Toth Z and Kalnay E 1997 Ensemble forecasting at NCEP and the breeding method *Mon. Weather Rev.* **125** 3297–319
[30] Trevisan A and Palatella L 2010 The extended Kalman filter and its reduction to the unstable subspace *Ecodyc 2010: Inf. Workshop on Exploring Complex Dynamics in High-Dimensional Chaotic Systems: From Weather Forecasting to Oceanic Flows (Dresden, Germany)* www.mpipks-dresden.mpg.de/~ecodyc10/Contributions/Trevisan.pdf
[31] Bannister R N 2008 A review of forecast error covariance statistics in atmospheric variational data assimilation. I: characteristics and measurements of forecast error covariances *Q. J. R. Meteorol. Soc.* **134** 1951–70
[32] Swanson K L, Palmer T N and Vautard R 2000 Observational error structures and the value of advanced assimilation techniques *J. Atmos. Sci.* **57** 1327–40
[33] Lorenz E N 1996 Predictability: a problem partly solved *Proc. Seminar on Predictability. European Center for Medium-Range Weather Forecasting (Shinfield Park, Reading, UK)* pp 1–18
[34] Thornton C L and Bierman G J 1976 A numerical comparison of discrete Kalman filtering algorithms: an orbit determination case study *JPL Tech. Memo.* **33** 771
[35] Hamill T M and Whitaker J S 2011 What constrains spread growth in forecasts initialized from ensemble Kalman filters? *Mon. Weather Rev.* **139** 117–31
[36] Carrassi A, Vannitsem S, Zupanski D and Zupanski M 2009 The maximum likelihood ensemble filter performances in chaotic systems *Tellus* **61** 587–600
[37] Bocquet M 2011 Ensemble Kalman filtering without the intrinsic need for inflation *Nonlinear Process. Geophys.* **18** 735–50
[38] Ng G-H C, McLaughlin D, Entekhabi D and Ahanin A 2011 The role of model dynamics in ensemble Kalman filter performance for chaotic systems *Tellus* A **63** 958–77
[39] Palatella L and Trevisan A 2012 Nonlinear stability of traffic models and the use of Lyapunov vectors for estimating the traffic state *Phys. Rev.* E submitted
[40] Orosz G, Krauskopf B and Wilson R E 2005 Bifurcations and multiple traffic jams in a car-following model with reaction time delay *Physica* D **211** 277–93